INTERNATIONAL JOURNAL FOR NUMERICAL METHODS IN FLUIDS, VOL. 6, 529–539 (1986)

BOUNDARY CONFORMED CO-ORDINATE SYSTEMS FOR SELECTED TWO-DIMENSIONAL FLUID FLOW PROBLEMS. PART II: APPLICATION OF THE BFG METHOD

J. HÄUSER

Department of Electrical and Mechanical Engineering, Am Lurtenhof 4, College of Landshut, 8300 Landshut, Germany

H. G. PAAP

Physikalisches Institut, NW II, University of Bayreuth, 8580 Bayreuth, Germany

D. EPPEL

Institute of Physics, GKSS-Research Center, 2054 Geesthacht, Germany

AND

S. SENGUPTA

Department of Mechanical Engineering, University of Miami, FL. 33124, U.S.A.

SUMMARY

This paper gives the results of an application of the SWEs (shallow water equations) to a part of the Hamburg harbour area, which is a complex flow domain, using the BFG approach, outlined in Part I. The results of a grid doubling procedure generating the desired computational grid from a coarse initial mesh are also presented. A second class of problems which is addressed, demands time-dependent co-ordinate systems. The problems which are solved are the free surface problem for a moving wave which eventually breaks and for a wave which is reflected by the solid walls of a rectangular basin.

KEY WORDS Shallow Water Equations Boundary Fitted Grids Time Dependent Solution Domains Free Surface Problems

INTRODUCTION

The present paper is concerned with the solution of fluid flow problems using boundary fitted co-ordinates. To show the use of BFGs for two-dimensional internal flows, several complex flow domains have been modelled. First, simulation results for a section of the Hamburg harbour area are presented. This area is geometrically very complex and is therefore well suited as an example demonstrating the capabilities of BFGs.

A second set of problems was calculated in order to see how time-dependent solution areas can be described. Two free surface problems were chosen, namely the breaking wave problem, first solved by Haussling,[1] and the reflection of a wave in a rectangular basin. Because of the boundary condition at the free surface, these problems are non-linear. When the wave begins to break, the grid is severely distorted and computations become meaningless.

0271–2091/86/080529–11$05.50

Received 1 February 1986
Revised 17 February 1986

SOLUTION OF THE SHALLOW WATER WAVE EQUATIONS

First, the SWEs are considered which describe the flow field and the water level in an inviscid rotating ocean under the assumption that the wavelength is much larger than the elevation from the still water level. In Cartesian co-ordinates the equations read

$$\begin{aligned} \frac{\partial u}{\partial t} + u\frac{\partial u}{\partial x} + v\frac{\partial u}{\partial y} - fv &= -g\frac{\partial h}{\partial x}, \\ \frac{\partial v}{\partial t} + u\frac{\partial v}{\partial x} + v\frac{\partial v}{\partial y} + fu &= -g\frac{\partial h}{\partial y}, \\ \frac{\partial h}{\partial t} + \frac{\partial (uD)}{\partial x} + \frac{\partial (vD)}{\partial y} &= 0, \end{aligned} \tag{1}$$

where u, v denote horizontal velocity components, h is water level and D is total water depth. If $\partial \mathbf{u}/\partial t \gg (\mathbf{u}\cdot\nabla)\mathbf{u}$ and $D \cong H$, equations (1) can be linearized by replacing D by H and omitting the convective terms.

Introduction of transports $U := uH$, $V := vH$ yields

$$\begin{aligned} \frac{\partial U}{\partial t} + gH\frac{\partial h}{\partial x} - fV &= 0, \\ \frac{\partial V}{\partial t} + gH\frac{\partial h}{\partial y} + fU &= 0, \\ \frac{\partial h}{\partial t} + \frac{\partial U}{\partial x} + \frac{\partial V}{\partial y} &= 0. \end{aligned} \tag{2}$$

Three initial conditions are necessary for equations (2). We choose initial conditions for U, V and h. For solid walls it is required that the normal velocity component vanishes, i.e. $U_{\hat{\mathbf{n}}} = 0$. For open boundaries, i.e. boundaries which separate the solution area from the rest of the ocean, no physical boundary conditions can be specified. Therefore, the transient water level h is prescribed. This requires, however, that open boundaries be separated far enough from each other so that inaccuracies of the measured water levels do not cause unrealistic flow fields.

If the boundary moves, we demand $\mathbf{u}D = \mathbf{0}$, which is satisfied for $D = 0$, i.e. the total water depth vanishes. This property can be used to determine the variation of the shoreline in the course of time. Hence dry running areas can also be modelled, e.g. Reference 2. The shallow water equations can be solved analytically for a rectangular basin of constant depth as well as for circular basins of constant and parabolic depth variation. Extensive comparisons of analytical and numerical results, along with comparisons between BFG models and conventional finite difference models using rectangular grids are found in Reference 3.

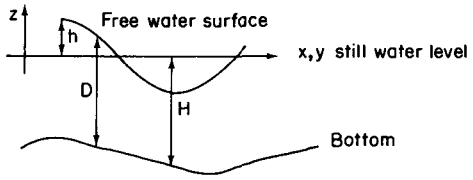

Figure 1. Co-ordinate system for shallow water equations: h = surface elevation; D = water depth; H = still water depth

Introducing the vectors $\mathbf{u}=(U,\ V,\ 0)^{\mathrm{T}}=(u_1,\ u_2,\ 0)^{\mathrm{T}}$ and $\mathbf{f}=(0,\ 0,\ f)^{\mathrm{T}}$, the momentum equations (2) can be written in the form

$$\frac{\partial u_i}{\partial t}+gH\frac{\partial h}{\partial x_i}+(\mathbf{f}\times\mathbf{u})_i=0, \tag{3}$$

or

$$u_{i,t}+gHh_{,i}+\hat{\varepsilon}_{ijk}f^j u^k=0,$$

where the nomenclature of section 3 of Part I[4] has been used. The respective covariant form is

$$u_{i,t}+gHh_{,i}+\sqrt{g}\hat{\varepsilon}_{ijk}f^j u^k=0, \tag{4}$$

where u_i, u^k are covariant and contravariant components. In generalized co-ordinates equations (2) take the following form, where the first two equations follow directly from (4) and the third one is obtained from (29) in Part I which gives the general form of the divergence:

$$\begin{aligned}
&\frac{\partial}{\partial t}g_{1i}u^i+gH\frac{\partial h}{\partial x_1}-\sqrt{g}fu^2=0,\\
&\frac{\partial}{\partial t}g_{2i}u^i+gH\frac{\partial h}{\partial x_2}+\sqrt{g}fu^1=0,\\
&\frac{\partial h}{\partial t}+u^i_{,i}=\frac{\partial h}{\partial t}+u^i_{,i}+\Gamma^i_{ik}u^k=0.
\end{aligned} \tag{5}$$

If one wishes to retain the Cartesian velocity components, equations (2) can be transformed by use of the chain rule, which yields

$$\begin{aligned}
&\frac{\partial U}{\partial t}+gH\frac{\partial h}{\partial x}-fV=\frac{\partial U}{\partial t}+gH\left(\frac{\partial h}{\partial \xi}\frac{\partial \xi}{\partial x}+\frac{\partial h}{\partial \eta}\frac{\partial \eta}{\partial x}\right)-fV=\\
&\frac{\partial U}{\partial t}+gH\frac{1}{J}(h_{,\xi}y_\eta-h_{,\eta}y_\xi)-fV\qquad=0,\\
&\frac{\partial V}{\partial t}+gH\frac{1}{J}(-h_{,\xi}x_\eta+h_{,\eta}x_\xi)+fU\qquad=0,\\
&\frac{\partial h}{\partial t}+\frac{1}{J}(U_{,\xi}y_\eta-U_{,\eta}y_\xi-V_{,\xi}x_\eta+V_{,\eta}x_\xi)=0.
\end{aligned} \tag{6}$$

Derivatives can be brought into a conservative form by adding a term $f(y_{\xi\eta}-y_{\eta\xi})=0$, where f is a function of x, e.g.

$$\begin{aligned}
\frac{\partial f}{\partial x}&=f_{,\xi}\xi_x+f_{,\eta}\eta_x=\frac{1}{J}(f_{,\xi}y_\eta-f_{,\eta}y_\xi)\\
&=\frac{1}{J}(f_{,\xi}y_\eta+fy_{\eta\xi}-fy_{\xi\eta}-f_{,\eta}y_\xi)=\frac{1}{J}[(fy_\eta)_{,\xi}-(fy_\xi)_{,\eta}],
\end{aligned} \tag{7}$$

where the first form is non-conservative and the second is the conservative one. For the analytical solution the two schemes are equivalent. Numerically the schemes are different, since, dependent on the discretization, the order of the derivation cannot be interchanged for second derivatives. In Reference 5 it was reported that a conservative scheme yields more accurate results. Test calculations for an annular ring revealed that in this case the non-conservative scheme was more accurate.[3] As a BC it is required that the normal transport component $U_{\hat{n}}$ vanishes at solid walls.

Since inviscid flow is considered, the tangential transport need not vanish. By use of equations (2), one obtains for $U_{\hat{\mathbf{t}}}$ and $U_{\hat{\mathbf{n}}}$

$$\frac{\partial U_{\hat{\mathbf{n}}}}{\partial t} + gH\frac{\partial h}{\partial \hat{\mathbf{n}}} - fU_{\hat{\mathbf{t}}} = 0,$$

$$\frac{\partial U_{\hat{\mathbf{t}}}}{\partial t} + gH\frac{\partial h}{\partial \hat{\mathbf{t}}} + fU_{\hat{\mathbf{n}}} = 0. \tag{8}$$

Since the staggered grid is chosen such that only velocity points lie on the boundary, the first of equations (8) is not needed. In order to calculate the Cartesian UV-components of the tangential transport, the angle ψ is introduced, which is the angle of rotation between the Cartesian x–y and the $\hat{\mathbf{t}}$–$\hat{\mathbf{n}}$ co-ordinate systems and is defined by

$$\hat{\mathbf{t}} = \frac{1}{\sqrt{(x'^2 + y'^2)}}\begin{pmatrix} x' \\ y' \end{pmatrix} = \begin{pmatrix} -\sin\psi \\ \cos\psi \end{pmatrix} \tag{9}$$

where the prime denotes the partial derivative with respect to either ξ or η, since boundary curves are parametrized by either variable. Hence, the equations on the boundary take the form

$$\frac{\partial U}{\partial t} + gH\sin\psi\left(\sin\psi\frac{\partial h}{\partial x} - \cos\psi\frac{\partial h}{\partial y}\right) = 0,$$

$$\frac{\partial V}{\partial t} - gH\cos\psi\left(\sin\psi\frac{\partial h}{\partial x} - \cos\psi\frac{\partial h}{\partial y}\right) = 0. \tag{10}$$

The above equations are discretized by replacing the time derivatives by forward differences, and the space derivatives by central differences. The discretized transformed SWEs are of the form

$$\frac{U_{i,j}^{n+1} - U_{i,j}^{n}}{\tau} + gH\frac{1}{J_{ij}}[y_{\eta i,j}(h_{i+1,j}^{n+1} - h_{i-1,j}^{n+1})/2 - y_{\xi i,j}(h_{i,j+1}^{n+1} - h_{i,j-1}^{n+1})/2] - fV_{i,j} = 0,$$

$$\frac{V_{i,j}^{n+1} - V_{i,j}^{n}}{\tau} - gH\frac{1}{J_{i,j}}[x_{\eta i,j}(h_{i+1,j}^{n+1} - h_{i-1,j}^{n+1})/2 - x_{\xi i,j}(h_{i,j+1}^{n+1} - h_{i,j-1}^{n+1})/2] + fU_{i,j} = 0,$$

$$\frac{h_{i,j}^{n+1} - h_{i,j}^{n}}{\tau} + \frac{1}{2J_{i,j}}[y_{\eta i,j}(U_{i+1,j}^{n} - U_{i-1,j}^{n}) - y_{\xi i,j}(U_{i,j+1}^{n} - U_{i,j-1}^{n}) - x_{\eta i,j}(V_{i+1,j}^{n} - V_{i-1,j}^{n}) + x_{\xi i,j}(V_{i,j+1}^{n} - V_{i,j-1}^{n})] = 0. \tag{11}$$

Under the assumption that a solution is formed by plane waves, the integration in time must not amplify the wave amplitudes, otherwise the scheme is unstable. Explicit schemes often have the advantage of smaller phase error in comparison with implicit schemes, but are limited by the allowable time-step size. In the following the results of the stability analysis for equations (11) are presented, where the error introduced by interpolation on the staggered grid of, e.g. $\partial U/\partial x$, to the location of an h-point is not accounted for. Furthermore, it is assumed that metric coefficients are locally constant. Inserting the plane wave formulation

$$\begin{pmatrix} U \\ V \\ h \end{pmatrix} = \begin{pmatrix} U_0 \\ V_0 \\ h_0 \end{pmatrix}\exp[\mathrm{i}(\omega t - kx - ly)] \tag{12}$$

in the discretized equations (11), denoting the grid spacing by Δ and assuming $f = 0$ (no Coriolis force), one finally obtains the dispersion relation for the explicit scheme (U and V values taken at time step n) where $\cos\omega\tau$ is replaced by $1 - \omega^2\tau^2/2$ (that is $\omega\tau \ll 1$ is assumed)

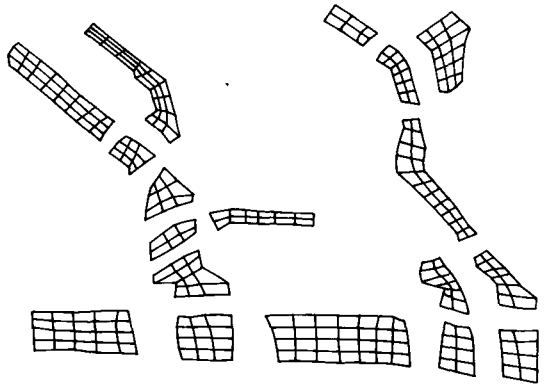

Figure 2. Exploded view of an 18 segment area which is part of the Hamburg harbour region. The shallow water wave equations for constant water depth have been solved on this solution domain

$$\omega \approx \frac{\sqrt{(gH)}}{\Delta}\sqrt{(g^{11}\sin^2 k\Delta + 2g^{12}\sin k\Delta \sin l\Delta + g^{22}\sin^2 l\Delta)}. \tag{13}$$

For the semi-implicit scheme, where U and V values are taken at time step $n+1$, the r.h.s. of equation (13) is multiplied by $\sqrt{2}$. In Cartesian co-ordinates the dispersion relations reduce (in the one-dimensional case) to the well-known formulae

$$\frac{\omega}{k} = \sqrt{(gH)}\left[1 - \frac{(k\Delta)^2}{6}\right]; \quad \frac{\omega}{k} = \sqrt{(2gH)}\left(1 - \frac{k^2\Delta^2}{6}\right) \tag{14}$$

for the explicit and semi-implicit schemes, respectively. Waves of wavelength 2Δ are stationary as observed from equation (14). Only waves of longer wavelength are propagated with a phase speed depending on the wavelength. A wave packet is therefore dispersed in the course of time. The case of strongly varying coefficients in space may invalidate the above analysis,[6] and refraction and reflection of waves must be expected. It is well known, that the order of a scheme is reduced for variable coefficients. Numerical errors grow with $1/\sin\theta$ where θ is the angle of intersection between co-ordinate lines. Large variations of the aspect ratio may have the same effect. Without proof, we state that the above scheme is unstable if the Coriolis terms are computed at time step n. If the values are taken at $n+1$, the scheme is stable provided the time step size is properly chosen.

Figure 2 depicts the segment structure of the initial grid for the Hamburg harbour area and in Figure 3 the effect of the grid doubling algorithm is shown.[14]

Although the stability analysis shows that the simple numerical scheme used is stable, and numerical experiences for an annular ring demonstrated the stability of the scheme even after 1000 periods,[3] the scheme became unstable for the complex Hamburg harbour area (Figure 4) after some 15,000 time steps, which is equivalent to 24 hours of simulation time. This is most likely due to the type of staggered grid used, since U, V values are computed at the same location. This scheme worked well in Reference 2 where the SWEs were solved on an annular ring with large Coriolis coefficients, and excellent agreement with the analytic solution was obtained. Problems with an implicit scheme are reported in Reference 7. Implicit schemes are much more laborious to program for composite grids, since larger overlaps are necessary.

The instability could not be eliminated by filtering,[8,9] although linear filtering was successfully used to damp the non-linear instabilities of the free surface problem (Figure 5) which arise from the non-linear boundary conditions. Since the free surface problem was described in Reference 1 and 10, it is only briefly discussed here.

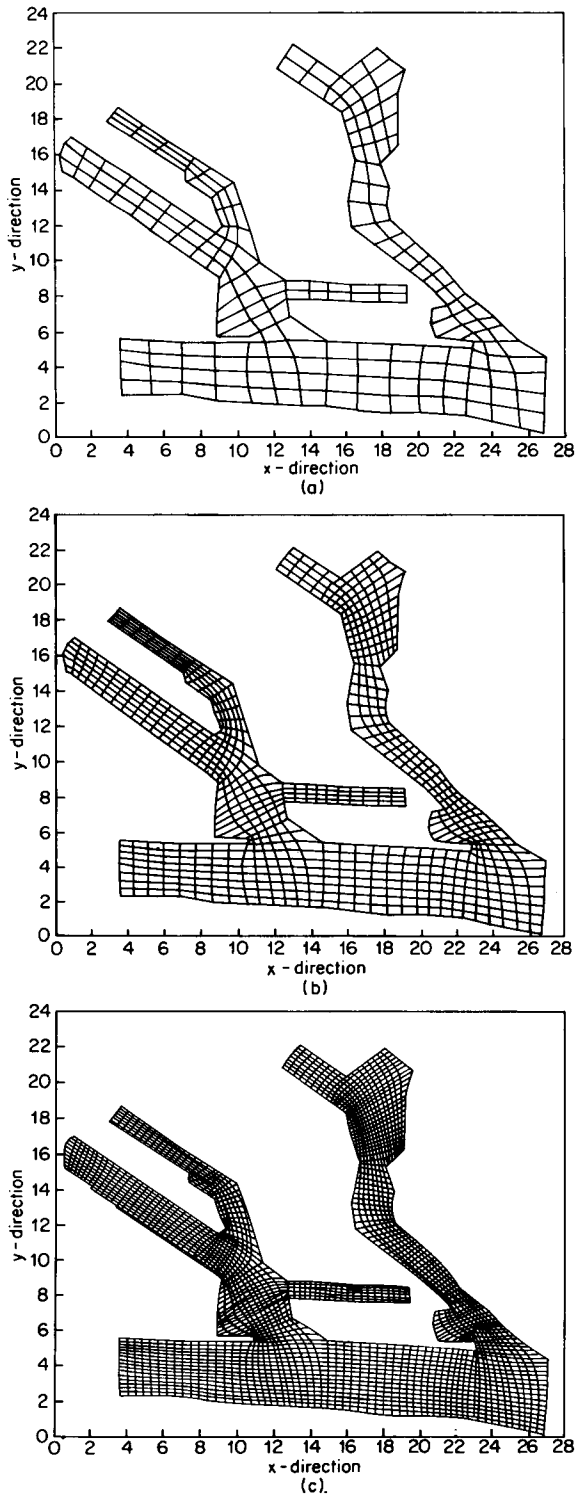

Figure 3.(a) Shows the initial coarse grid for the Hamburg harbour area; (b) refined grid after first doubling; (c) final grid

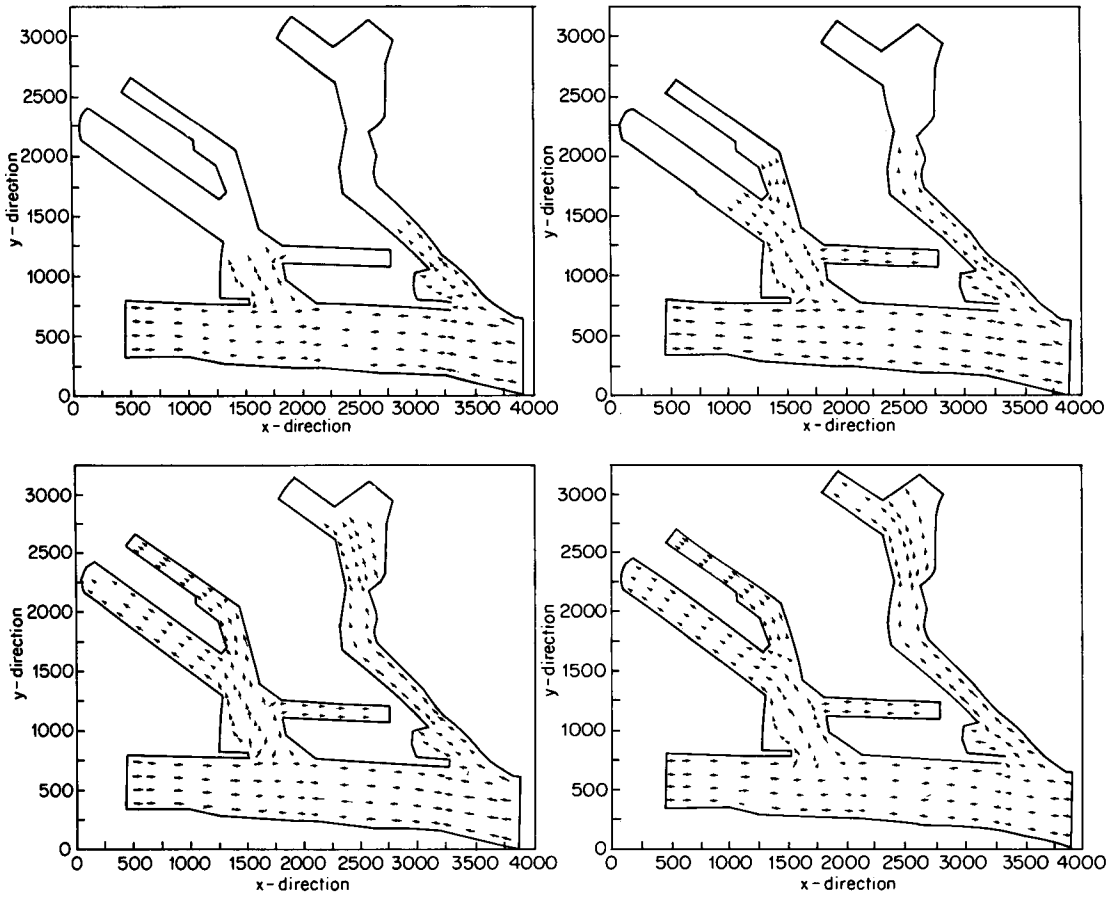

Figure 4. Calculated flow field for a part of the Hamburg harbour area. It was assumed that the solution area is of constant depth. This, however, does not simplify the equations since variable coefficients are introduced by the transformation

To simplify the continuity and momentum equations, we assume the fluid to be incompressible and inviscid. It is further assumed that the fluid is irrotational. Since the rotation of a gradient always vanishes, a velocity potential ϕ can be introduced, where $\mathbf{v} = \nabla\phi$. Insertion into the continuity equation leads to Laplace's equation

$$\Delta\phi = 0. \tag{15}$$

The velocity potential has to satisfy the following BCs:

(i) At solid boundaries: $V_n = \nabla\phi \cdot \mathbf{n} = 0$ where $\mathbf{n}$ is the unit normal vector. (16)

(ii) At the free surface (dynamical BC): since the interface (water–air) has no mass, the forces, i.e. the pressures at both sides, must be equal; hence $p = p_0$ where p_0 is (constant) air pressure. If the Euler equations are solved for p and $\nabla \times \mathbf{v} = 0$ is used, this yields

$$\frac{\partial\phi}{\partial t} = -\tfrac{1}{2}(\nabla\phi \cdot \nabla\phi) + gz, \qquad \text{on} \quad S \text{ (free surface)}, \tag{17}$$

where p_0 was set to zero and gz accounts for gravity.

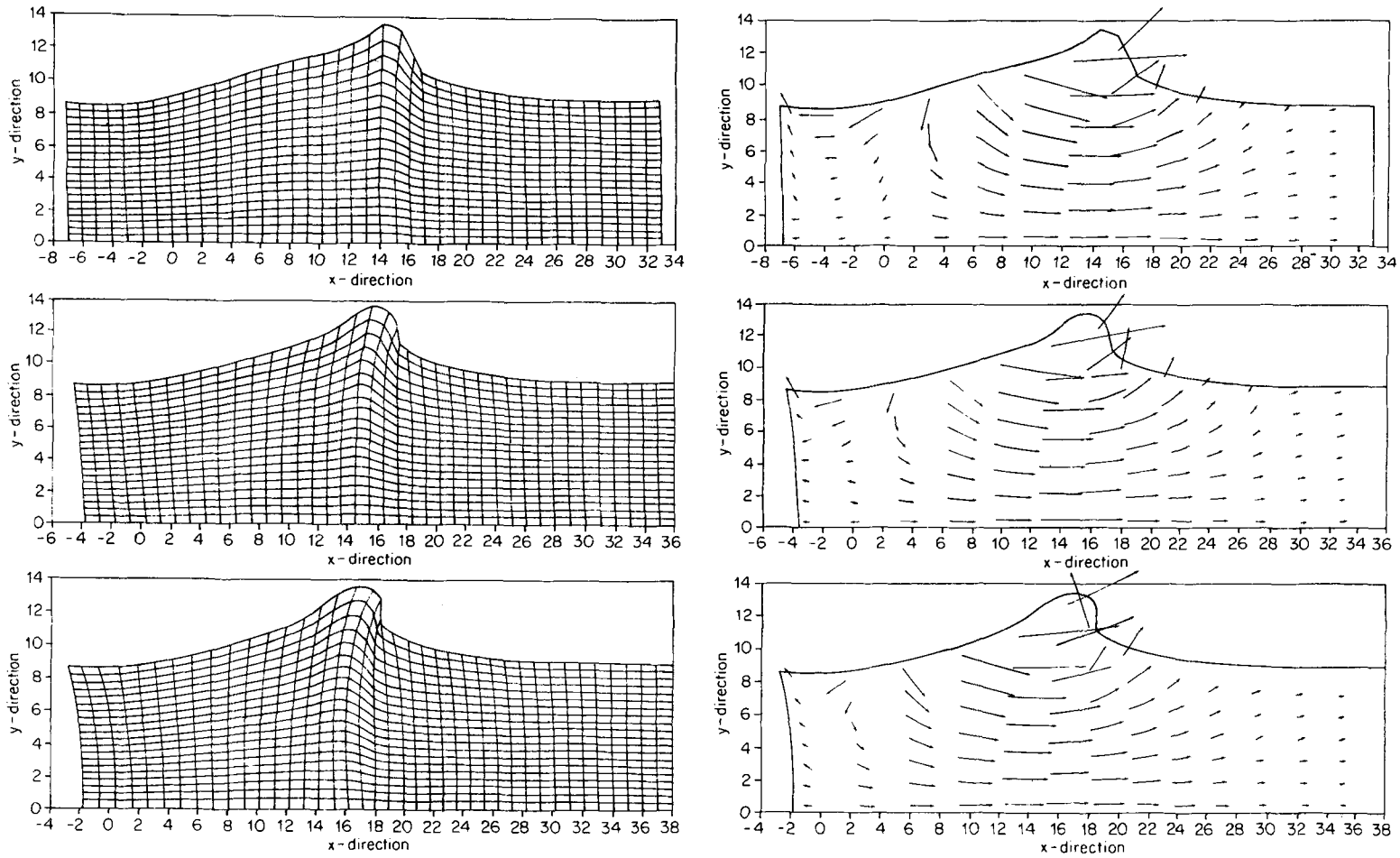

Figure 5. Free surface problem with time-dependent BFGs and respective flow fields. The calculations cannot be carried on when the wave starts to break since the grid is severely distorted. In the above example the co-ordinate system moves to the right with a constant velocity which corresponds to the average wave speed. As initial condition a soliton solution is chosen in order to ensure that the left and right boundaries of the solution area are not influenced

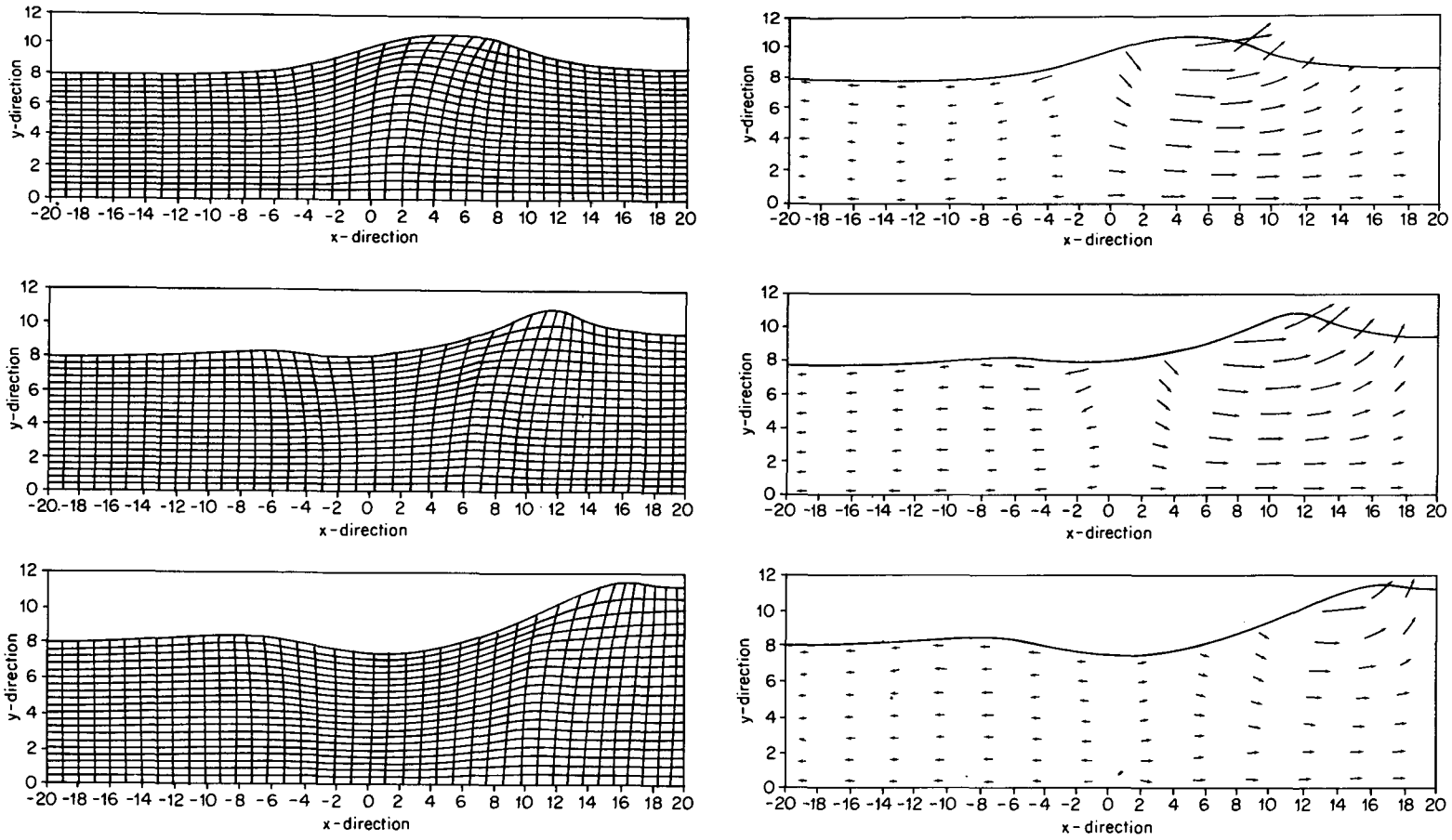

Figure 6. Reflection of water waves by solid walls at left and right boundaries. It is mandatory that at these walls Neumann BCs are employed for the solution of the grid generation equations in order that grid points can move with the water level

(iii) At left and right sides (see Figure 5): constant velocities are prescribed, since the co-ordinate system moves with velocity $\mathbf{v}_s$ with respect to the bottom of the solution domain. This condition prevents the wave running out of the solution area

$$\nabla\phi = -\mathbf{v}_s. \tag{18}$$

(iv) Computation of the location of unknown free surface: the free surface is defined by the property that fluid does not cross it, i.e. the normal velocity component of the fluid with respect to the free surface must be equal to the normal velocity component of the moving free surface. After some algebraic manipulation this finally leads to the (obvious) result

$$d\mathbf{x}/dt = \nabla\phi, \qquad \text{on} \quad S, \tag{19}$$

where $\mathbf{x}$ is the position vector of a fluid particle on the free surface.

(v) The grid is generated from

$$\Delta\xi = P; \qquad \Delta\eta = Q \qquad + \text{BCs}. \tag{20}$$

Although the Laplace equation has to be solved, the problem is non-linear because of the above BCs.

Along with (i)–(iv), the transformed grid generation equations indicated in (v), (Part I, equations (47) and (48)) have to be solved. The BCs for this system are obtained from the computed co-ordinates resulting from the wave movement.

In Figure 6, where the reflection of a wave by solid walls is considered, Dirichlet conditions are not allowed for the grid generation equations at left and right boundaries. Rather, Neuman conditions have to be prescribed such that boundary points can move with the water level.

For the transformation of the above equations the time dependence (Part I, equations (32)) has to be accounted for. In the computational plane, the co-ordinate system is fixed.

The computations are performed in the following order. First, initial distributions for the velocity potential ϕ and the free surface are needed. Here the solution of the Korteweg–de Vries equation is used[11] which describes a soliton and gives expressions for the surface elevation h and for ϕ on the free surface. The initial distributions for ϕ as well as for ξ and η are found by numerical integration using the respective equations. The solution has the advantage that it represents only a small peak, so that BC (iii) is satisfied. Of course, the soliton solution is not stable since in our case the full non-linear equations are solved.

From (iv) the new shape and location of the free surface are determined and from the dynamical BCs (ii) the new velocity potential ϕ at the free surface is found.

Employing this new geometry, the new co-ordinate system is constructed solving the equations in (v). With that, $\Delta\phi = 0$ can be solved along with the BCs (i) and (iii). After that, the next time step can be calculated.

CONCLUSIONS AND OUTLOOK

In this paper a description of the use of BFGs is given along with the application of these techniques to three time-dependent problems in CFD. As an example problem in this paper the application of the BFG method to the SWEs for a complex two-dimensional solution domain was studied. Stability problems were encountered after some 15,000 time steps for the explicit scheme. It is believed that the instability is caused by the type of staggered grid used. The instability was not removed by linear filtering.

It will be tested whether predictor–corrector schemes as, for example, described in Reference 12

will yield better results for the SWEs. Since these schemes are in delta form, the use of a multigrid method could be considered.

Two non-linear problems with time dependent geometry, namely the breaking wave problem and the reflection of a wave by solid walls were successfully modelled, demonstrating that BFGs are capable of handling complex flow domains.

ACKNOWLEDGEMENT

The authors are grateful for NATO research grant 681/84 and also for support by GKSS-Research-Center.

This paper is dedicated to the 85th birthday of Prof. W. Hanle, I. Physikalisches Institut, Universität Giessen, Germany.

REFERENCES

1. H. J. Haussling, 'Solution of nonlinear water wave problems using boundary-fitted coordinate systems', in J. F. Thomson (ed.) *Numerical Grid Generation*, North Holland, 1982, pp. 385–408.
2. P. Petersen *et al.*, 'An error minimizing scheme for the nonlinear shallow water equations with moving boundaries', in C. Taylor (ed.), *Numerical Methods in Nonlinear Problems*, Pineridge Press, 1983, pp. 826–836.
3. J. Häuser, H. G. Paap, D. Eppel and A. Mueller, 'Solution of shallow water equations for complex flow domains via boundary fitted coordinates', *Int. numer. methods fluids*, **5**, 727–744 (1985).
4. J. Häuser, H. G. Paap, D. Eppel and S. Sengupta, 'Boundary conformed coordinate systems for selected two-dimensional fluid flow problems'. Part I: generation of BFGs, *Int. j. numer. methods fluids*, **6**, 507–527 (1986).
5. B. H. Johnson, 'Numerical modelling of estuarine hydrodynamics on a boundary fitted coordinate systems', in J. F. Thomson (ed.) *Numerical Grid Generation*, North Holland, 1982, pp. 409–436.
6. C. W. Mastin, 'Error induced by coordinate systems', in J. F. Thomson (ed.) *Numerical Grid Generation*, North Holland, 1982, pp. 31–40.
7. B. H. Johnson, 'Numerical modelling of free surface hydrodynamics on curvilinear grids', in J. F. Thomson (ed.) *Short Course on Numerical Grid Generation*, Mississippi State University, 1984.
8. R. Shapiro, 'Linear filtering', *Mathematics of Computation*, **29**, (132), 1094–1097 (1975).
9. M. Y. Hussaini, *et al.*, 'Spectral methods for the Euler equations. Part I—Fourier methods and shock capturing', *AIAA Journal*, **33**, (1), 64–70 (1985).
10. H. G. Paap, 'Lösung der Zweidimensionalen Navier–Stokes Gleichungen mit Hilfe randangepaßter Koordinaten', *Diploma Thesis*, Universität Hamburg, 1984.
11. G. L. Lamb, Jr., *Elements of Soliton Theory*, Wiley, 1980. Chapter 6.
12. R. W. MacCormack, 'A numerical method for solving the equations of compressible flow', *AIAA 19th Aerospace Sciences Meeting*, AIAA-81-0110, 1981.
13. W. C. Thacker, 'Irregular grid finite difference techniques: simulations of oscillations in shallow circular basins', *J. Phys. Ocean.*, **7**, 282–292 (1977).
14. H. G. Paap, J. Häuser, D. Eppel, 'Automatic grid doubling for composite meçhes', in *Proceedings of the Sixth GAMN Conference on Numerical Methods in Fluid Mechanics*, Vieweg and Sohn, Braunsohweig, 279–286, 1986.